AIP Publishing

This manuscript was accepted by J. Chem. Phys. Click here to see the version of record.

Effect of chain stiffness on the entropic segregation of chain ends to the surface of a polymer melt

S. Blaber,[1] P. Mahmoudi,[2] R. K. W. Spencer,[1] and M. W. Matsen[1,2,3,*]

[1]*Department of Physics & Astronomy,*

[2]*Department of Chemical Engineering,*

and [3]*Waterloo Institute for Nanotechnology,*

University of Waterloo, Waterloo, Ontario N2L 3G1, Canada

(Dated: November 22, 2018)

Abstract

Entropic segregation of chain ends to the surface of a monodisperse polymer melt and its effect on surface tension is examined using self-consistent field theory (SCFT). In order to assess the dependence on chain stiffness, the SCFT is solved for worm-like chains. Our focus is still on relatively flexible polymers, where the persistence length of the polymer, ℓ_p, is comparable to the width of the surface profile, ξ, but still much smaller than the total contour length of the polymer, ℓ_c. Even this small degree of rigidity causes a substantial increase in the level of segregation, relative to that of totally flexible Gaussian chains. Nevertheless, the long-range depletion that balances the surface excess still exhibits the same universal shape derived for Gaussian chains. Furthermore, the excess continues to reduce the surface tension by one unit of k_BT per chain end, which results in the usual N^{-1} reduction in surface tension observed by experiments. This enhanced segregation will also extend to polydisperse melts, causing the molecular-weight distribution at the surface to shift towards smaller N_n relative to the bulk. This provides a partial explanation for recent quantitive differences between experiments and SCFT calculations for flexible polymers.

ACCEPTED MANUSCRIPT

AIP Publishing

This manuscript was accepted by J. Chem. Phys. Click here to see the version of record.

I. INTRODUCTION

Silberberg[1] has cleverly argued that the surface of a polymer melt behaves like a reflecting boundary. This, in turn, implies that the probability distributions of the individual segments of the polymer are uniform all the way from the bulk right up to the surface. It also implies that the surface tension should be independent of molecular weight or rather the degree of polymerization, N. However, simulations,[2–6] self-consistent field theory (SCFT),[7–10] and experiments[11] all find an excess of chain ends at the surface. Furthermore, SCFT[7–10] and experiments[12–18] report an N-dependence in the surface tension. Other deviations from Silberberg's hypothesis have also been detected by simulations.[19,20]

The deviations can be attributed to the fact that the Silberberg argument is based on a couple of simplifying assumptions, an off-lattice model in which the energy of a polymer configuration is unaffected when folded about a plane and an infinitely-sharp surface profile. Previous predictions of entropic segregation either represented polymers on a lattice,[6] used a bead-spring model where folding causes a change in energy,[5,9] or involved a surface profile of finite width.[7] It has been shown that the finite width of the surface profile generally provides the dominant contribution to the segregation.[21,22] Excluded-volume interactions will also affect the energy of folding a polymer configuration and could, therefore, contribute to entropic segregation. However, simulations[23] have shown that this effect is relatively minor, presumably because hard-core interactions are, to a good approximation, screened in polymer melts.[24]

Because the number of chain ends has to be conserved on the molecular length scale (i.e., two per molecule), the excess at the surface is balanced by depletion of equivalent magnitude extending into the melt a distance of order $aN^{1/2}$, the end-to-end length of a polymer. An analytical approximation[9] for flexible Gaussian chains predicts that the compensating depletion takes the form

$$\delta\phi_e(z) \approx \frac{A}{N^{1/2}} B\left(\frac{z}{aN^{1/2}}\right) , \tag{1}$$

involving the universal function

$$\begin{aligned} B(\zeta) \;=\; & \sqrt{\frac{6}{\pi}} \exp\left(-\frac{3}{2}\zeta^2\right) \\ & -\frac{1}{\pi}\int_{-\infty}^{\infty} dk_\zeta \frac{(e^{-x}-1)^2 e^{ik_\zeta \zeta}}{e^{-x}+x-1} , \end{aligned} \tag{2}$$

ACCEPTED MANUSCRIPT

AIP Publishing

This manuscript was accepted by J. Chem. Phys. Click here to see the version of record.

where $x = k_\zeta^2/6$. The amplitude of the effect, A, is dependent upon the microscopic details of the system. The segregation also causes a reduction in surface tension,[9]

$$\frac{\gamma_{\rm en}}{a\rho_0 k_B T} \approx \Gamma_\infty - \frac{2A}{N} \ , \tag{3}$$

from the infinite molecular-weight limit, Γ_∞, that is proportional to A. This proportionality results because each chain end that segregates to the surface reduces the free energy by one unit of $k_B T$.[10,25]

Experiments[11] have claimed to observe the entropic segregation using neutron reflectivity on polystyrene chains with deuterated ends. However, this claim is not entirely conclusive, because deuterium labeling is know to create enthalpic interactions strong enough to mask entropic effects.[26,27] Nevertheless, the segregation has also been detected in polydisperse melts,[32] where it causes a shift in the molecular-weight distribution towards smaller N_n at the surface relative to the bulk, due to the fact that shorter polymers have more ends per unit volume.[21,23,28–31] In this case, the experiments measured the shift in N_n using MALDI time-of-flight spectrometry, which does not require any labeling. Although the shift was in qualitative agreement with SCFT, the effect was considerably stronger than predicted. Two possible explanations were given. It was suggested that the shift may have been enhanced by enthalpic effects.[12,33] Even without labeling, the interactions of end segments will generally differ somewhat from those of middle segments.[34] The other suggestion was that the difference could be related to chain stiffness not captured by the SCFT calculations, which were based on freely-jointed chains. Chain stiffness penalizes the folding of polymer chains, which violates the Silberberg assumptions and thus could contribute to the entropic segregation.[21]

Here, we extend the previous SCFT for entropic segregation and its effect on surface tension to semiflexible worm-like chains.[35] Still, our study focuses on relatively flexible polymers, where the persistence length, ℓ_p, is comparable to the width of the surface, ξ, but still much smaller than the total contour length of the polymer, ℓ_c. The coefficients A and Γ_∞ are calculated from results for the long-chain limit, and then the accuracy of Eq. (1) for the compensating depletion and Eq. (3) for the molecular-weight dependence of the surface tension are tested for polymers of finite length.

ACCEPTED MANUSCRIPT

AIP Publishing

This manuscript was accepted by J. Chem. Phys. Click here to see the version of record.

II. THEORY

We consider a monodisperse melt of n polymers, each containing N segments of length b, giving a total contour length of $\ell_c = bN$. The configuration of the α'th molecule is specified by the space curve $\mathbf{r}_\alpha(s)$, where the backbone parameter runs from $s = 0$ to 1. The polymers are modeled as worm-like chains,[35,36] for which the energy of a polymer configuration is given by

$$\frac{E}{k_B T} = \frac{\kappa}{2N} \int_0^1 ds \, |\mathbf{u}'_\alpha(s)|^2 , \tag{4}$$

where

$$\mathbf{u}_\alpha(s) \equiv \mathbf{r}'_\alpha(s)/l_c \tag{5}$$

is a unit vector tangent to the chain. The parameter κ is a dimensionless bending modulus, which controls the persistence length, $\ell_p = b\kappa$. In a bulk melt, the average end-to-end length of a worm-like chain is[35–37]

$$R_0 = \sqrt{2\ell_p(\ell_c - \ell_p[1 - \exp(-\ell_c/\ell_p)])} \ . \tag{6}$$

For long chains of $\ell_c \gg \ell_p$, this expression reduces to $R_0 \approx a\sqrt{N}$, where the statistical segment length is $a = \sqrt{2\ell_p b}$. Note that we follow the convention where segments are defined to have a specified volume, ρ_0^{-1}, such that the total volume of the melt is $V = nN/\rho_0$.

Using this model, we examine a flat surface of area $\mathcal{A}$ located at $z = 0$. To make the problem tractable, the molecular interactions are represented by a static field, $w(z)$, which depends only on the coordinate z normal to the surface. Within this mean-field approximation, the polymer concentration relative to the bulk is

$$\phi(z) = \frac{V}{2Q} \int_{-1}^1 du_z \int_0^1 ds \, G(z, u_z, s) G(z, -u_z, 1-s) \ , \tag{7}$$

where

$$Q = \frac{\mathcal{A}}{2} \int_{-1}^1 du_z \int dz \, G(z, u_z, s) G(z, -u_z, 1-s) \tag{8}$$

is a single-chain partition function. Note that the integration in Eq. (8) is independent of s.

The above expressions involve the propagator, $G(z, u_z, s)$, which is the partition function for a chain fragment of sN segments with one end constrained such that the projections of $\mathbf{r}_\alpha(s)$ and $\mathbf{u}_\alpha(s)$ onto the z-axis are z and u_z, respectively. It satisfies the differential

ACCEPTED MANUSCRIPT

AIP Publishing

This manuscript was accepted by J. Chem. Phys. Click here to see the version of record.

ergration

$$\frac{\partial G}{\partial s} = \frac{l_c}{2l_p}\frac{\partial}{\partial u_z}\left[(1-u_z^2)\frac{\partial G}{\partial u_z}\right] - l_c u_z \frac{\partial G}{\partial z} - wG \ , \tag{9}$$

with the initial condition $G(z, u_z, 0) = 1$.[36,37] The equation is solved with reflecting boundary conditions, using the numerical algorithm described in Ref. 38. We ensure that the grid sizes used in the algorithm are sufficiently small and that the boundaries at negative and positive z are sufficiently far from the surface (i.e., $z = 0$) such that numerical inaccuracies are irrelevant on the scale of our plots.

Generally, one needs to specify the interaction energy of the melt, which is typically written as

$$U[\phi] = \int d\mathbf{r} f(\phi) \ , \tag{10}$$

where $f(\phi)$ is the energy density relative to the bulk (i.e., $f(1) = 0$). In SCFT, the field is normally adjusted to satisfy the self-consistent condition, $w(z) = Nf'(\phi(z))/\rho_0 k_B T$. As such, the problem of evaluating the surface segregation is coupled to the calculation of the surface profile, $\phi(z)$. Past studies[7,8] have used a simple choice for $U[\phi]$ that results in some unphysical behaviors, which we will discuss later. Rather than dealing with the complication of a more realistic $U[\phi]$,[39–41] we take the alternative approach of adjusting $w(z)$ in order to create a specified concentration profile.[9,10,21] We specifically choose the sigmoidal profile,

$$\phi(z) = \frac{1}{2}\left[1 + \tanh\left(\frac{2z}{\xi}\right)\right] \ , \tag{11}$$

characteristic of simulations,[42,43] where the width of the surface, ξ, is used as our unit of length. The field is determined with the same Anderson mixing algorithm[44] used previously.[10,21]

As usual, the SCFT is unaffected by an additive constant to the field, and so for convenience we set $w(z) = 0$ in the bulk. With this choice, $G(z, u_z, s) \to 1$ as $z \to \infty$, and thus Eq. (7) requires $\mathcal{Q} = V$ in order that $\phi(z) \to 1$ as $z \to \infty$. Given this requirement, the dimensionless concentration of chain ends relative to the bulk is

$$\phi_e(z) = \frac{1}{2}\int_{-1}^{1} du_z G(z, u_z, 1) \ , \tag{12}$$

and the surface tension is[45]

$$\gamma_{\text{en}} = -\frac{\rho_0 k_B T}{N}\int dz\, w(z)\phi(z) \ . \tag{13}$$

ACCEPTED MANUSCRIPT

AIP Publishing

This manuscript was accepted by J. Chem. Phys. Click here to see the version of record.

Because our calculation creates the surface by constraining the polymer concentration instead of using molecular interactions, it only provides the entropic contribution to the surface tension, $\gamma_{\rm en}$. This is also true of calculations that use constraining walls to create the surface.[28,30,46] The enthalpic contribution is given by $\gamma_{\rm int} = U[\phi]/\mathcal{A}$. Although $\gamma_{\rm int}$ contains no explicit N-dependence, it does produce an implicit N-dependence due to variations in $\phi(z)$, which are, in principle, determined by minimizing the total tension, $\gamma = \gamma_{\rm int} + \gamma_{\rm en}$, with respect to $\phi(z)$. Nevertheless, we will illustrate later that $\gamma_{\rm en}$ alone provides the correct N-dependence to leading order (i.e., to order N^{-1}).

The analytical Eqs. (1) and (3) are derived from an expansion about the long-chain limit.[9] The propagator for this limit, $G_\infty(z,u_z)$, is obtained by integrating Eq. (9) until it becomes independent of s, or in other words until both sides of the equation equal zero.[47] The field is then adjusted as before, but using the simpler expression

$$\phi(z) = \frac{V}{2\mathcal{Q}} \int_{-1}^{1} du_z G_\infty(z,u_z) G_\infty(z,-u_z) \ , \tag{14}$$

where

$$Q = \frac{\mathcal{A}}{2} \int_{-1}^{1} du_z \int dz\, G_\infty(z,u_z) G_\infty(z,-u_z) \ . \tag{15}$$

Once the propagator, $G_\infty(z,u_z)$, and the corresponding field, $w_\infty(z)$, have been determined, the coefficients in Eqs. (1) and (3) are given by

$$A = \frac{1}{a} \int dz [\phi_{e,\infty}(z) - \phi(z)] \ , \tag{16}$$

where

$$\phi_{e,\infty}(z) = \frac{1}{2} \int_{-1}^{1} du_z\, G_\infty(z,u_z) \tag{17}$$

is the concentration of ends relative to the bulk, and

$$\Gamma_\infty = -\frac{b}{a l_c} \int dz\, w_\infty(z) \phi(z) \ . \tag{18}$$

III. RESULTS

We begin by considering the long-chain limit (i.e., $\ell_c \to \infty$). Figure 1(a) compares the distribution of chain ends, $\phi_{e,\infty}(z)$, to the overall polymer concentration, $\phi(z)$, for several different persistence lengths, ℓ_p. In all cases, there is an excess of chain ends near the surface

ACCEPTED MANUSCRIPT

AIP Publishing

This manuscript was accepted by J. Chem. Phys. Click here to see the version of record.

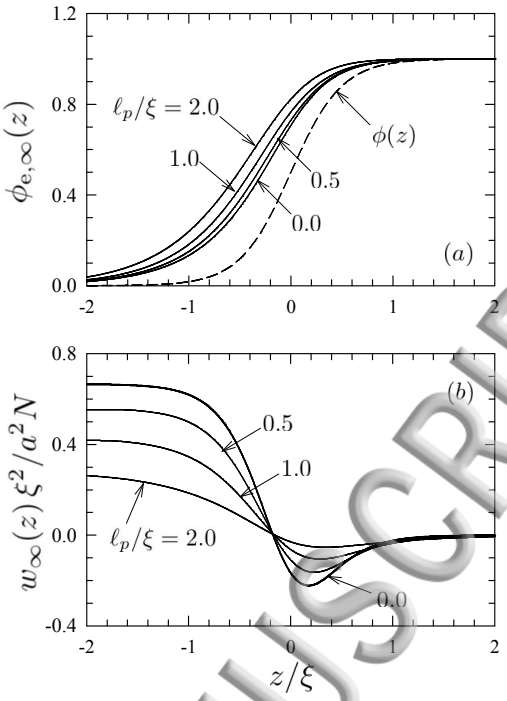

FIG. 1: (a) Concentration of chain ends, $\phi_{e,\infty}(z)$, and (b) self-consistent field, $w_\infty(z)$, calculated in the long-chain limit (i.e., $\ell_c \to \infty$) for different persistence lengths, ℓ_p. The $\ell_p = 0$ curves are given by Eqs. (19) and (20). The dashed curve in (a) denotes the total polymer concentration, $\phi(z)$.

[i.e., $\phi_{e,\infty}(z) > \phi(z)$]. For flexible Gaussian chains (i.e., $\ell_p = 0$), the distribution obeys the simple expression[7,21]

$$\phi_{e,\infty}(z) = \sqrt{\phi(z)}\ . \tag{19}$$

As the polymers become more rigid, $\phi_{e,\infty}(z)$ extends further from the surface. Figure 1(b) shows the field, $w_\infty(z)$, required to enforce the surface profile, $\phi(z)$. It involves a shallow well that pulls the polymers toward $z = 0$ followed by a barrier that prevents them from invading the $z < 0$ region. The field for flexible Gaussian chains, which is given by[48]

$$w_\infty(z) = \frac{a^2 N \nabla^2 \sqrt{\phi(z)}}{6\sqrt{\phi(z)}}\ , \tag{20}$$

needs to counteract the loss of configurational entropy,[48]

$$\Delta S_{\rm conf} = -\frac{k_B a^2 \rho_0}{24} \int d\mathbf{r} \frac{|\nabla\phi|^2}{\phi}\ , \tag{21}$$

which acts to oppose gradients in $\phi(z)$. This free energy penalty diminishes as the polymers become more rigid, which, in turn, explains the reduction in the field strength with increasing

ACCEPTED MANUSCRIPT

AIP Publishing

This manuscript was accepted by J. Chem. Phys. Click here to see the version of record.

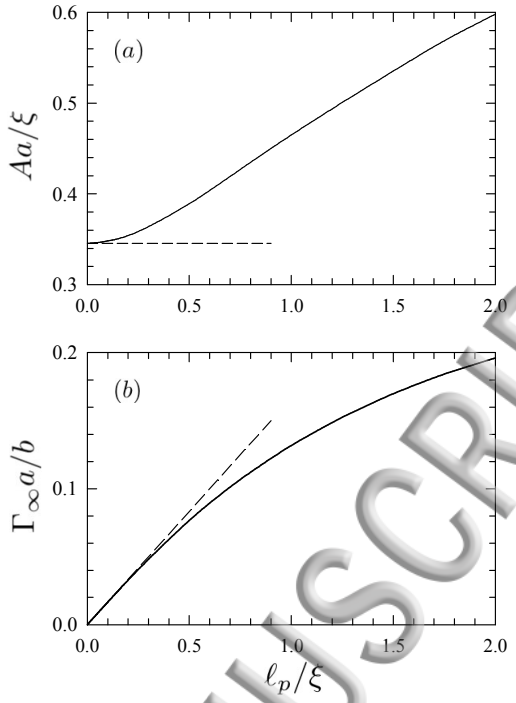

FIG. 2: (a) Dimensionless surface excess of chain ends, A, and (b) dimensionless surface tension, Γ_∞, as a function of persistence length, ℓ_p, calculated in the long-chain limit. The dashed lines denote the Gaussian-chain predictions in Eqs. (22) and (23).

ℓ_p.

Figure 2(a) shows the integrated excess of chain ends, A, defined in Eq. (16). For persistence lengths, ℓ_p, comparable to the width of the surface profile, ξ, there is about a 40% increase relative to the dashed line for flexible Gaussian chains,[21]

$$A = \frac{\xi \ln 2}{2a} \ , \tag{22}$$

which is obtained by inserting Eqs. (11) and (19) into Eq. (16). Figure 2(b) shows the dimensionless surface tension, Γ_∞, defined in Eq. (3) and calculated from Eq. (18). The dashed line denotes the Gaussian-chain approximation,[21]

$$\Gamma_\infty = \frac{a}{12\xi} \ , \tag{23}$$

obtained by inserting Eqs. (11) and (20) into Eq. (18). In all cases, the tension is smaller than that of flexible Gaussian chains of equal segment length. Note that the quantities, A and Γ_∞, in Fig. 2 will appear later as coefficients in the analytical expressions for the compensating depletion, Eq. (1), and surface tension, Eq. (3), of finite chains.

ACCEPTED MANUSCRIPT

AIP Publishing

This manuscript was accepted by J. Chem. Phys. Click here to see the version of record.

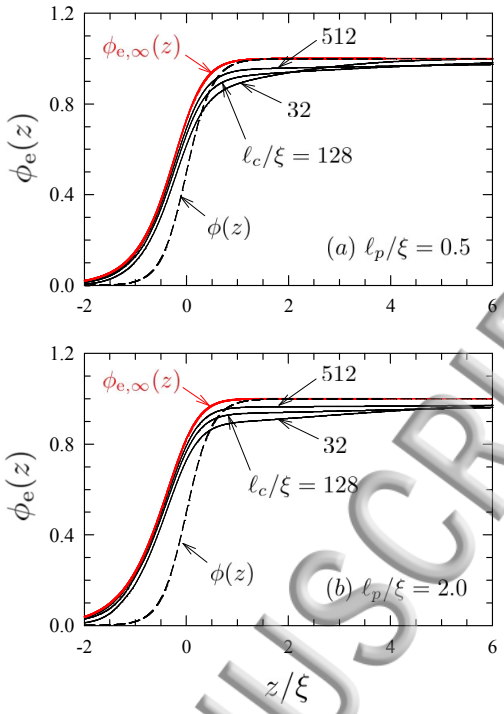

FIG. 3: Concentration of chain ends, $\phi_e(z)$, calculated for persistence lengths of (a) $\ell_p = \xi/2$ and (b) $\ell_p = 2\xi$. As the contour length, ℓ_c, increases, the profiles converge to the long-chain limit, $\phi_{e,\infty}(z)$, from Fig. 1(a). The dashed curves denote the total polymer concentration, $\phi(z)$.

We now turn our attention to polymers of finite size. Figure 3 compares the distribution of chain ends, $\phi_e(z)$, to the total polymer concentration, $\phi(z)$, for a range of chain lengths, ℓ_c. As required, $\phi_e(z)$ converges to the infinite-chain limit, $\phi_{e,\infty}(z)$, but rather slowly. Finite-chain effects are still significant even for our longest polymers of $\ell_c = 512\xi$. One important qualitative difference of finite chains is that $\delta\phi_e(z) \equiv \phi_e(z) - \phi(z)$ switches from positive (i.e., an excess of ends) for $z \lesssim 0$ to negative (i.e., a depletion of ends) for $z \gtrsim 0$. This is because the excess of ends at the surface has to come from somewhere, and consequently a compensating depletion occurs just beyond the surface. As illustrated in Fig. 3, the depletion becomes smaller in amplitude and extends further into the melt for longer polymers. The depletion eventually vanishes as $\ell_c \to \infty$, simply because ends from larger polymers can be extracted from ever deeper into the melt.

As shown previously for flexible chains,[9,10,23] Fig. 4 illustrates that the amplitude of the depletion decreases as R_0^{-1} while the range increases as R_0. Furthermore, Fig. 4 illustrates that, as the polymers increase in size, the depletion approaches the analytical result in Eq.

ACCEPTED MANUSCRIPT

AIP Publishing

This manuscript was accepted by J. Chem. Phys. Click here to see the version of record.

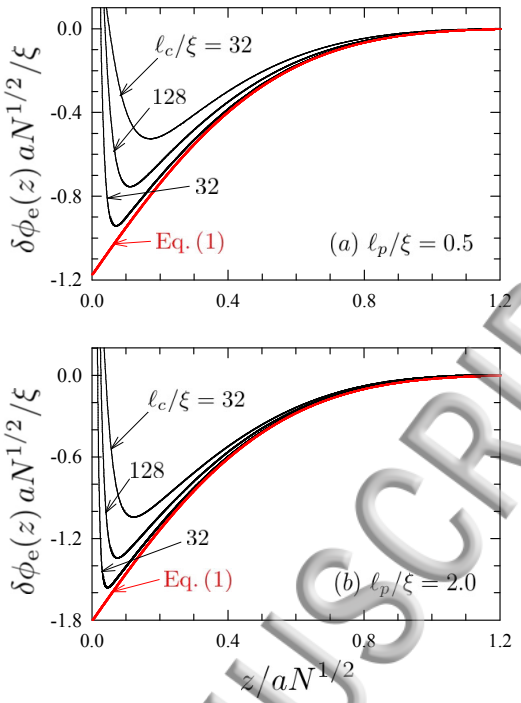

FIG. 4: Long-range depletion of chain ends, $\delta\phi_e(z) \equiv \phi_e(z) - \phi(z) < 0$, scaled with respect to the average end-to-end length, $aN^{1/2}$, plotted for persistence lengths of (a) $\ell_p = \xi/2$ and (b) $\ell_p = 2\xi$. As the contour length, ℓ_c, increases, the profiles converge to the universal shape in Eq. (1).

(1), involving the universal shape, $B(z/aN^{1/2})$, with an amplitude given by the same A plotted in Fig. 1(a). Although the persistence length does not affect the shape of the depletion, it does have a sizeable effect on the amplitude. Indeed, the amplitude is approximately 50% larger for $\ell_p = 2\xi$ than for $\ell_p = \xi/2$.

We conclude by examining the effect of finite chain length on the surface tension. Figure 5(a) plots the entropic contribution to the surface tension, $\gamma_{\rm en}$, as a function of chain length, $\ell_c = bN$. The symbols represent numerical SCFT calculations, while the lines denote the analytical approximation in Eq. (3). This confirms the N^{-1} dependence observed in experiments for high molecular-weight polymers.[12–18] Just as in experiments, the decrease in tension becomes more gradual for shorter polymers. In fact, the empirical fit to $N^{-2/3}$ obtained by experiments[14–17,49,50] for oligomers is accurately reproduced by our shortest four polymers, as illustrated in Fig. 5(b). However, as we will explain later, this is not the true power-law behavior of small molecules.

ACCEPTED MANUSCRIPT

AIP Publishing

This manuscript was accepted by J. Chem. Phys. Click here to see the version of record.

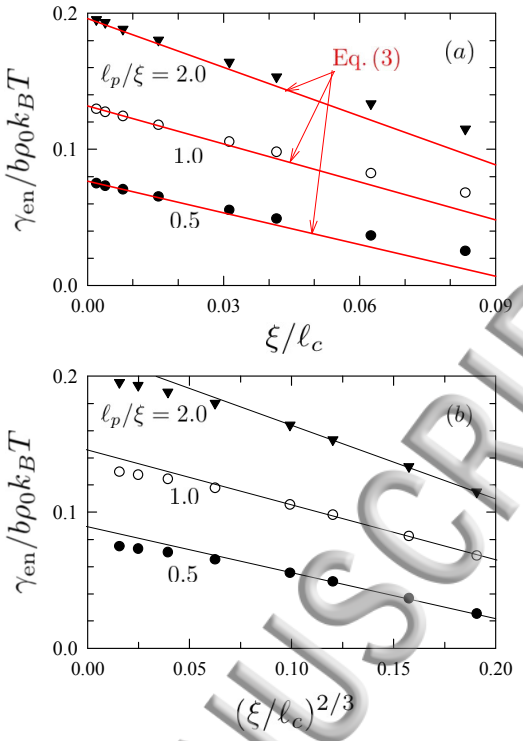

FIG. 5: Reduction in surface tension, $\gamma_{\rm en}$, for three different persistence lengths, ℓ_p, plotted versus (a) $\ell_c^{-1} \propto N^{-1}$ and (b) $\ell_c^{-2/3} \propto N^{-2/3}$. The lines in (a) denote the analytical approximation in Eq. (3), while the lines in (b) are fits to the four shortest polymers.

IV. DISCUSSION

The SCFT for Gaussian chains relies on the assumption that the field, $w(z)$, changes slowly on the scale of the segment length, a. However, polymer surfaces are relatively narrow, and consequently even flexible polymers generally do not satisfy this criterion at a surface. Therefore, it becomes necessary to use a less coarse-grained model such as that of worm-like chains. Although the introduction of small degrees of chain stiffness, on the scale of the surface profile, does not change the shape of the long-range depletion plotted in Fig. 4, it does have a substantial effect on the level of surface segregation in Fig. 1(a) and the amplitude of the depletion in Fig. 2(a).

The shift in the molecular-weight distribution at the surface of polydisperse melts observed by Hill *et al.*[32] is a direct consequence of the segregation of chains ends. Thus, it follows that our predicted increase in the entropic segregation accounts for a significant portion of the discrepancy between the experimental measurements and the SCFT for flexible

ACCEPTED MANUSCRIPT

AIP Publishing

This manuscript was accepted by J. Chem. Phys. Click here to see the version of record.

chains.[51] The remaining discrepancy could very well be attributed to small differences in the interactions of end segments relative to middle segments.[34] If known, this enthalpic effect could readily be included in the SCFT calculation. It would, to a good approximation, simply alter the values of A and Γ_∞.[7,30,46]

Figure 5 suggests that surface tension increases with persistent length, while Fig. 2(b) illustrates that the tension is lower than that of flexible Gaussian chains (denoted by the dashed line). It is important to realize that the generalization from Gaussian to worm-like chains introduces an additional length scale; there are two independent lengths, ℓ_p and b, rather than just $a = \sqrt{2\ell_p b}$. Consequently, the tension is affected by both the persistence length and the cross-sectional area of the polymer, $1/b\rho_0$, which is controlled by b given the convention of defining segments based on a common volume, ρ_0^{-1}. At constant ℓ_p and ℓ_c, the surface tension depends linearly on the number of molecules per unit area, which is inversely proportional to the cross-sectional area. This simple dependence is scaled out of the results in Fig. 5, and thus the comparison is effectively between polymers of the same cross-sectional area. On the other hand, the conclusion that the tension is lower relative to Gaussian chains applies when comparing molecules with equal statistical segment lengths.

The $N^{-2/3}$ dependence suggested by Fig. 5(b) is not, in fact, the true scaling behavior of short molecules. Once $\ell_c \lesssim \ell_p$, the degrees of freedom of each molecule are effectively reduced to five, three for its center of mass and two for its orientation. Furthermore, the orientation becomes random at the surface as the size of the molecule becomes comparable to the width of the surface (i.e., $R_0 \lesssim \xi$). Thus, the entropic contribution to the surface tension of short polymers reduces to that of translational entropy, which implies

$$\frac{\gamma_{\rm en}}{b\rho_0 k_B T} \approx \frac{1}{\ell_c}\int dz\, \phi(z) \ln \phi(z) = -0.4112\frac{\xi}{\ell_c}\ . \qquad (24)$$

This again results in an N^{-1} dependence, but with a smaller amplitude relative to the long-chain limit in Eq. (3). Interestingly, there are recent experiments[18] that show a crossover from one N^{-1} power-law at large N to another at small N. However, the convergence of our SCFT results in Fig. 5 to Eq. (24) occurs around $\ell_c \approx \xi$, which is well beyond the point where we can ignore the N-dependence of $\phi(z)$. Nevertheless, these SCFT results do emphasize the danger in accepting the previous empirical evidence for $N^{-2/3}$ scaling.[14–17,49,50]

At small N, the enthalpic part of the surface tension, $\gamma_{\rm int} = U[\phi]/\mathcal{A}$, contributes to the N-dependence of the total surface tension, $\gamma = \gamma_{\rm int} + \gamma_{\rm en}$, as a result of variations in $\phi(z)$.

ACCEPTED MANUSCRIPT

AIP Publishing

This manuscript was accepted by J. Chem. Phys. Click here to see the version of record.

Provided N is not too small, we can assume the profile changes affinely with N (i.e., its shape remains approximately constant while the width, ξ, varies). Given this assumption,

$$\frac{\gamma_{\text{int}}}{a\rho_0 k_B T} = \frac{c_1 \xi}{a} \ , \tag{25}$$

where c_1 is a constant determined by the shape of the polymer profile. If we also assume Gaussian chains, then Eqs. (3), (19) and (20) imply

$$\frac{\gamma_{\text{en}}}{a\rho_0 k_B T} = \frac{c_2 a}{\xi} - \frac{2c_3 \xi}{aN} \ , \tag{26}$$

where c_2 and c_3 are again constants determined by the shape of $\phi(z)$. Minimization of $\gamma = \gamma_{\text{int}} + \gamma_{\text{en}}$ with respect to ξ gives

$$\xi = \xi_\infty \left(1 + \frac{c_3}{c_1 N}\right) \tag{27}$$

to order N^{-1}, where $\xi_\infty = a\sqrt{c_2/c_1}$ is the width for infinitely-large polymers. Note that the broadening of the surface for finite polymers is consistent with simulation.[42] In any case, the resulting equilibrium tension is given by

$$\frac{\gamma}{a\rho_0 k_B T} = 2\Gamma_\infty - \frac{2A}{N} \tag{28}$$

to order N^{-1}, where $\Gamma_\infty = c_2 a/\xi_\infty$ and $A = c_3 \xi_\infty / a$ are the same constants in Eq. (3). Thus, the tension of infinitely-long polymers is split equally between enthalpy and entropy. This precise balance happens because $\gamma_{\text{int}} \propto \xi$ and $\gamma_{\text{en}} \propto \xi^{-1}$ in the infinite-chain limit, and thus the result is specific to Gaussian chains. More importantly, the $2A/N$ correction is exactly the same as that of γ_{en} in Eq. (3). This just relies on the fact that γ_{int} and γ_{en} for infinite chains are increasing and decreasing functions of ξ, respectively, and thus the conclusion that γ_{en} provides the leading-order molecular-weight dependence holds more generally.

The enthalpic contribution to the tension, γ_{int}, will, nevertheless, become important at small N. First of all, the higher-order (e.g., N^{-2}) corrections to γ will be affected by variations in the width, ξ. Second of all, our assumption that $\phi(z)$ changes affinely will breakdown at some point. For instance, a vapor phase will eventually occur,[52] and thus $\phi(z)$ will no longer vary between 0 and 1. Therefore, we cannot comment on the N-dependence of the total surface tension, γ, beyond the N^{-1} correction for long chains, without considering $U[\phi]$.

ACCEPTED MANUSCRIPT

AIP Publishing

This manuscript was accepted by J. Chem. Phys. Click here to see the version of record.

including $U[\phi]$ not only allows predictions at small N, it also allows one to relate ξ to the fundamental parameters of the molecular interactions and the polymer molecules. Wu *et al.*[7] did so using an energy density of

$$f(\phi) = -\frac{\nu\rho_0^2}{2}(\phi - 1)^2 \ , \tag{29}$$

where the excluded-volume parameter, ν, is directly related to the bulk compressibility. Naturally, the simple parabolic penalty for deviations from bulk density will be quantitatively inaccurate when $\phi(z)$ drops to zero, but there are also some qualitative failings.[10] The underlying problem is that the quadratic approximation causes the melt to behave like a gas, filling all available space. As a consequence, Ref. 7 had to impose a wall at $z = 0$ in order to create their surface. Although this produced a reasonable looking surface profile for continuous Gaussian chains, it results in a discontinuous profile for discrete chains.[8] The shortcomings are also evident from the fact that Wu *et al.* predicted a narrowing of the surface profile for decreasing N, which contradicts the common-sense behavior predicted in Eq. (27) and observed in simulations.[42] Of course, the problem can be remedied by using a more realistic $U[\phi]$ from, for example, density functional theory,[39–41] but that is beyond the scope of this paper.

V. SUMMARY

We have examined the effect of chain stiffness on the entropic segregation of chain ends to a polymer surface and the resulting consequence on surface tension. This was done by applying SCFT to a melt of worm-like chains. To avoid specifying the molecular interactions, $U[\phi]$, we simply constrained the surface to a sigmoidal concentration profile, $\phi(z)$, where the width, ξ, was treated as a system parameter. Although this only allowed us to evaluate the entropic contribution to surface tension, $\gamma_{\rm en}$, this was, nevertheless, sufficient to obtain the dominant (i.e., N^{-1}) molecular-weight dependence for the total surface tension, γ.

The focus of this study was on persistence lengths, ℓ_p, comparable to ξ but small relative to the overall contour length of the polymer, $\ell_c = bN$. For these relatively flexible polymers, the universal behavior of the compensating depletion in Eq. (1) and the resulting reduction in surface tension in Eq. (3) derived for Gaussian chains still holds. The finite stiffness does, however, cause a sizeable increase in the amplitude A and a modest decrease in the

ACCEPTED MANUSCRIPT

AIP Publishing

This manuscript was accepted by J. Chem. Phys. Click here to see the version of record.

cient Γ_∞, relative to the Gaussian-chain predictions in Eqs. (22) and (23), respectively. Interestingly, the molecular-weight dependence of the surface tension for our shortest chains is consistent with the empirical fit from experiments to an $N^{-2/3}$ power-law. However, we emphasize that this behavior is not a true scaling relationship.

Our results have direct implications for polydisperse melts, where short polymers segregate to the surface because they have more ends per unit volume. As a consequence, the molecular-weight distribution is shifted towards a smaller average polymerization, N_n, relative to the bulk distribution. Our finding that chain stiffness significantly enhances entropic segregation helps account for the larger shifts measured in experiments relative to previous SCFT predictions based on flexible polymers.[32]

Acknowledgments

We thank Mark Foster, Josh McGraw, and Dave Morse for useful discussions. This work was supported by NSERC of Canada and computer resources were provided by SHARCNET of Compute Canada.

---

* Electronic address: mwmatsen@uwaterloo.ca

[1] A. Silberberg, J. Colloid Interface Sci. **90**, 86 (1982).

[2] S. K. Kumar, M. Vacatello, and D. Y. Yoon, J. Chem. Phys. **89**, 5206 (1988).

[3] A. Yethiraj and C. K. Hall, Macromolecules **23**, 1865 (1990).

[4] S. K. Kumar, M. Vacatello, and D. Y. Yoon, Macromolecules **23**, 2189 (1990).

[5] I. Bitsanis and G. Hadziioannou, J. Chem. Phys. **92**, 3827 (1990).

[6] R. S. Pai-Panandike, J. R. Dorgan, and T. Pakula, Macromolecules **30**, 6348 (1997).

[7] D. T. Wu, G. H. Fredrickson, J.-P. Carton, A. Ajdari, and L. Leiber, J. Polym. Sci., Part B **33**, 2373 (1995).

[8] M. Müller, B. Steinmüller, K.C. Daoulas, A Ramírez-Hernández, J.J. de Pablo, Phys. Chem. Chem. Phys. **13**, 10491 (2011).

[9] M. W. Matsen and P. Mahmoudi, Eur. Phys. J. E **37**, 78 (2014).

[10] P. Mahmoudi and M. W. Matsen, Eur. Phys. J. E **39**, 78 (2016).

ACCEPTED MANUSCRIPT

AIP Publishing

This manuscript was accepted by J. Chem. Phys. Click here to see the version of record.

[11] W. Zhao, X. Zhao, M. H. Rafailovich, J. Sokolov, R. J. Composto, S. D. Smith, M. Satkowski, T. P. Russell, W. D. Dozier, and T. Mansfield, Macromolecules **26**, 561 (1993).

[12] C. Jalbert, J.T. Koberstein, I. Yilgor, P. Gallagher, and V. Krukonis, Macromolecules **26**, 3069 (1993).

[13] G. T. Dee and B. B. Sauer, Macromolecules **26**, 2771 (1993).

[14] B. B. Sauer and G. T. Dee, Macromolecules **24**, 2124 (1991).

[15] B. B. Sauer and G. T. Dee, J. Coll. Interf. Sci. **162**, 25 (1994).

[16] B. B. Sauer and G. T. Dee, Macromolecules **27**, 6112 (1994).

[17] G. T. Dee and B. B. Sauer, Adv. Phys. **47**, 161 (1998).

[18] G. T. Dee and B. B. Sauer, J. Appl. Polym. Sci. **134**, 44431 (2017).

[19] M. Müller, J. Phys. Chem. **116**, 9930 (2002).

[20] A. Cavallo, M. Müller, J.P. Wittmer, A. Johner, K. Binder, J. Phys.: Conds. Matter **17**, S1697 (2005).

[21] P. Mahmoudi and M. W. Matsen, Eur. Phys. J. E **40**, 85 (2017).

[22] Reference 10 suggests that chain discreteness has a comparable effect to that of the surface profile when $\xi \sim a$, but Ref. 21 has shown otherwise.

[23] P. Mahmoudi, R. W. S. Forrest, T. M. Beardsley and M. W. Matsen, Macromolecules **51**, 1242 (2018).

[24] J. P. Wittmer, A. Cavallo, H. Xu, J. E. Zabel, P. Poliüska, N. Schulmann, H. Meyer, J. Fatago, A. Johner, S. P. Obukhov, and J. Baschnagel, J. Stat. Phys. **145**, 1017 (2011).

[25] Given that the excess of chain ends matches the depletion, the excess per unit area equals the bulk chain-end density, $2\rho_0/N$, times the integral $\int dz\,|\delta\phi_e(z)| = aA$, which is evaluated using Eqs. (1) and (2). It then follows that the finite-N correction for $\gamma_{\rm en}$ in Eq. (3) equals k_BT times the excess of ends per unit area.

[26] T. P. Russell, Annu. Rev. Mater. Sci. **21**, 249 (1991).

[27] A. Hariharan, S. K. Kumar, and T. P. Russell J. Chem. Phys. **98**, 4163 (1993).

[28] A. Hariharan, S. K. Kumar, and T. P. Russell, Macromolecules **23**, 3584 (1990).

[29] J. van der Gucht, N. A. M. Besseling, and G. J. Fleer, Macromolecules **35**, 6732 (2002).

[30] V. S. Minnikanti, Z. Qian, and L. A. Archer, J. Chem. Phys. **126**, 144905 (2007).

[31] C. Y. Teng, Y. J. Sheng, and H. K. Tsao, Soft Matter **12**, 4603 (2016).

[32] J. A. Hill, K. J. Endres, P. Mahmoudi, M. W. Matsen, C. Wesdemiotis, and M. D. Foster, ACS

ACCEPTED MANUSCRIPT

AIP Publishing

This manuscript was accepted by J. Chem. Phys. Click here to see the version of record.

Macro Lett. **7**, 487 (2018).

[33] J. H. Jang, R. Ozisik, and W. L. Mattice, Macromolecules **33**, 7663 (2000).

[34] P. G. de Gennes, C. R. Acad. Sci. Paris **307**, 1841 (1988).

[35] O. Kraty and G. Porod, Recl. Trav. Chim. **68**, 1106 (1949).

[36] N. Saito, K. Takahashi, and Y. Yunoki, J. Phys. Soc. Jpn. **22**, 219 (1967)

[37] G. H. Fredrickson, *The Equilibrium Theory of Inhomogeneous Polymers*, (Oxford University Press, New York, 2006).

[38] K. C. Daoulas, D. N. Theodorou, V. A. Harmandaris, N. C. Karayiannis, and V. G. Mavrantzas, Macromolecules **38**, 7134 (2005).

[39] S. K. Nath, J. D. McCoy, J. P. Donley, and J. G. Curro, J. Chem. Phys. **103**, 1635 (1995).

[40] F. Schmid, J. Chem. Phys. **104**, 9191 (1996).

[41] F. Schmid, J. Phys.: Condens. Matter **10**, 8105 (1998).

[42] K. C. Daoulas, V. A. Harmandaris, and V. G. Mavrantzas, Macromolecules **38**, 5780 (2005).

[43] A. V. Lukyanov and A. E. Likhtman, J. Chem. Phys. **138**, 034712 (2013).

[44] D. G. Anderson, J. Assoc. Comput. Mach. **12**, 547 (1965).

[45] Note that the field differs by a factor of N/k_BT from the definition used for discrete chains in Refs. 9, 10, and 21.

[46] V. S. Minnikanti and L. A. Archer, Macromolecules **39**, 7718 (2006).

[47] D. C. Morse and G. H. Fredrickson, Phys. Rev. Lett. **73**, 3235 (1994).

[48] M. W. Matsen, in *Soft Matter, Vol. 1: Polymer Melts and Mixtures*, edited by G. Gompper, M. Schick (Wiley-VCH, Weinheim, 2006).

[49] G. L. Gaines, J. Phys. Chem. **73**, 3143 (1969).

[50] D. G. LeGrand and G. L. Gaines, J. Polym. Sci. **45**, C34 (1971).

[51] Reference 21 shows that the value of A for freely-jointed polymers is virtually identical to that of Gaussian chains for the values of ξ considered in Ref. 32.

[52] S. Zhu, Y. Chai, and J. A. Forrest, Phys. Rev. Materials **1**, 025605 (2017).

ACCEPTED MANUSCRIPT

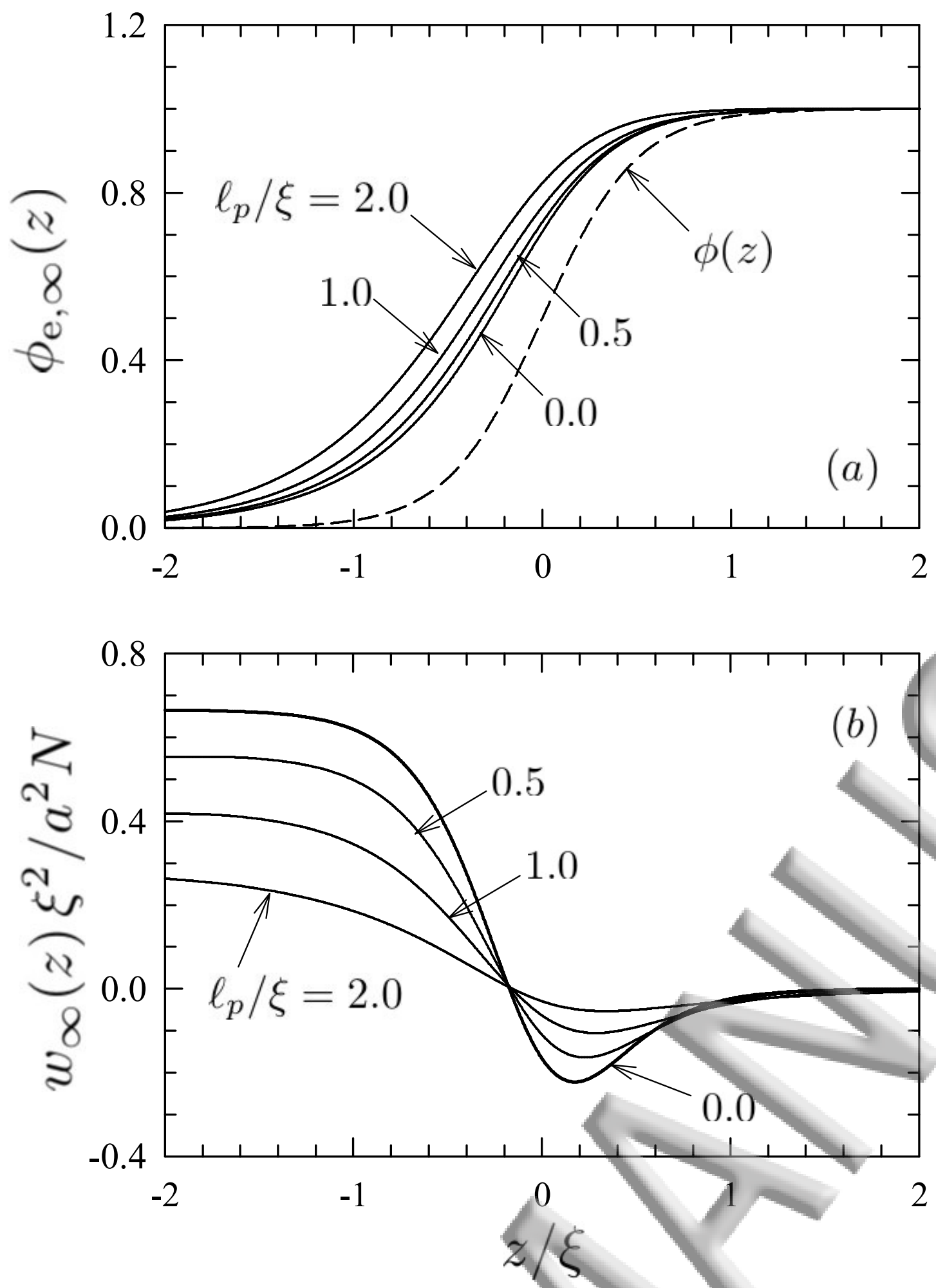
1.2
0.8
0.4
0.0
-2
-1
0
1
2
$\phi_{e,\infty}(z)$
$\ell_p/\xi = 2.0$
1.0
0.5
0.0
$\phi(z)$
(a)
0.8
0.4
0.0
-0.4
$w_\infty(z)\,\xi^2/a^2N$
(b)
0.5
1.0
$\ell_p/\xi = 2.0$
0.0
z/ξ

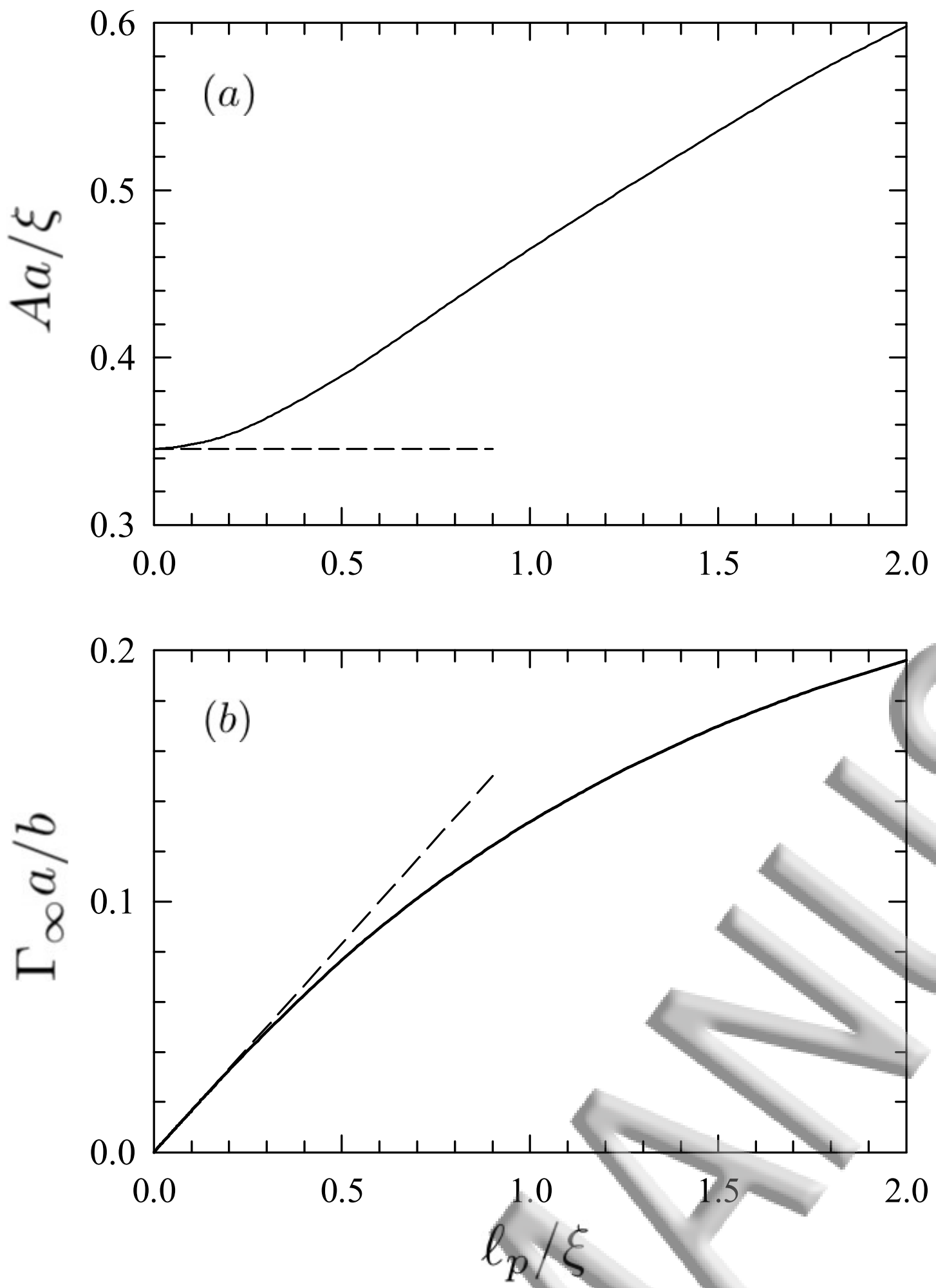
(a)
Aa/ξ
0.6
0.5
0.4
0.3
0.0
0.5
1.0
1.5
2.0
(b)
$\Gamma_\infty a/b$
0.2
0.1
0.0
0.0
0.5
1.0
1.5
2.0
ℓ_p/ξ

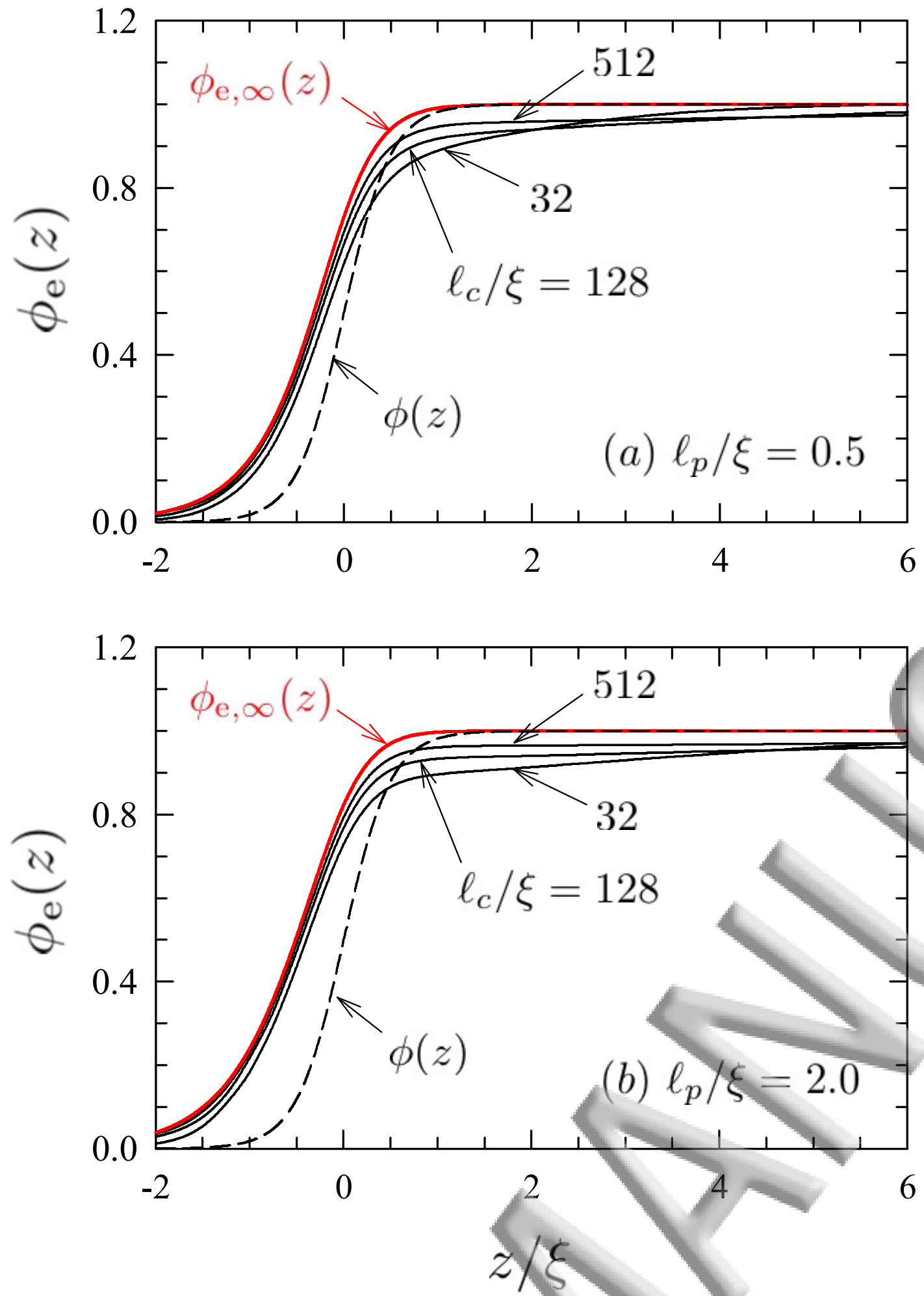
1.2
0.8
0.4
0.0
-2
0
2
4
6
$\phi_{\mathrm{e}}(z)$
$\phi_{\mathrm{e},\infty}(z)$
512
32
$\ell_c/\xi = 128$
$\phi(z)$
$(a)\ \ell_p/\xi = 0.5$
$(b)\ \ell_p/\xi = 2.0$
z/ξ

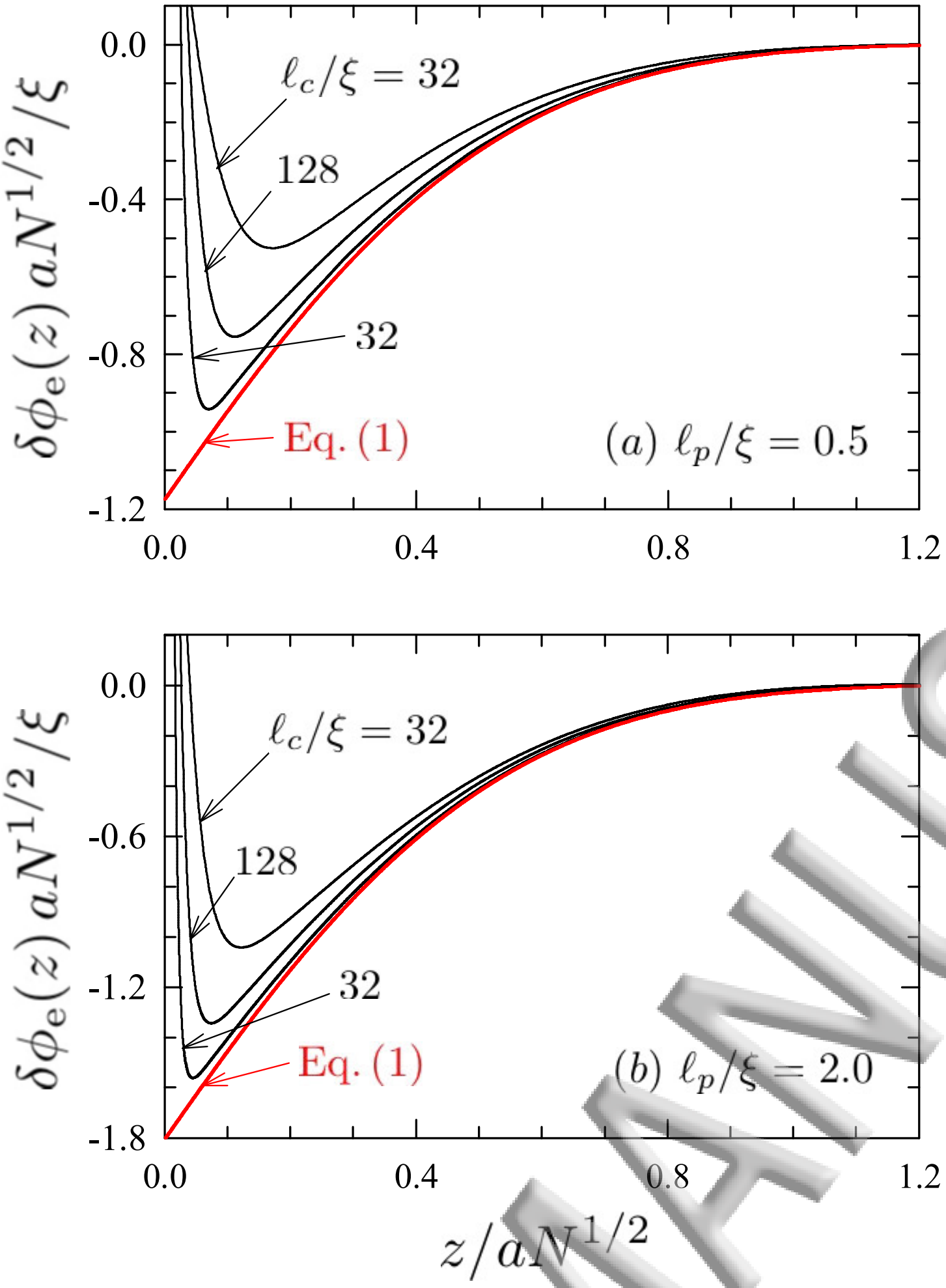
0.0
-0.4
-0.8
-1.2
$\ell_c/\xi = 32$
128
32
Eq. (1)
$(a)\ \ell_p/\xi = 0.5$
$\delta\phi_e(z)\, aN^{1/2}/\xi$
0.0
0.4
0.8
1.2
0.0
-0.6
-1.2
-1.8
$\ell_c/\xi = 32$
128
32
Eq. (1)
$(b)\ \ell_p/\xi = 2.0$
$\delta\phi_e(z)\, aN^{1/2}/\xi$
0.0
0.4
0.8
1.2
$z/aN^{1/2}$

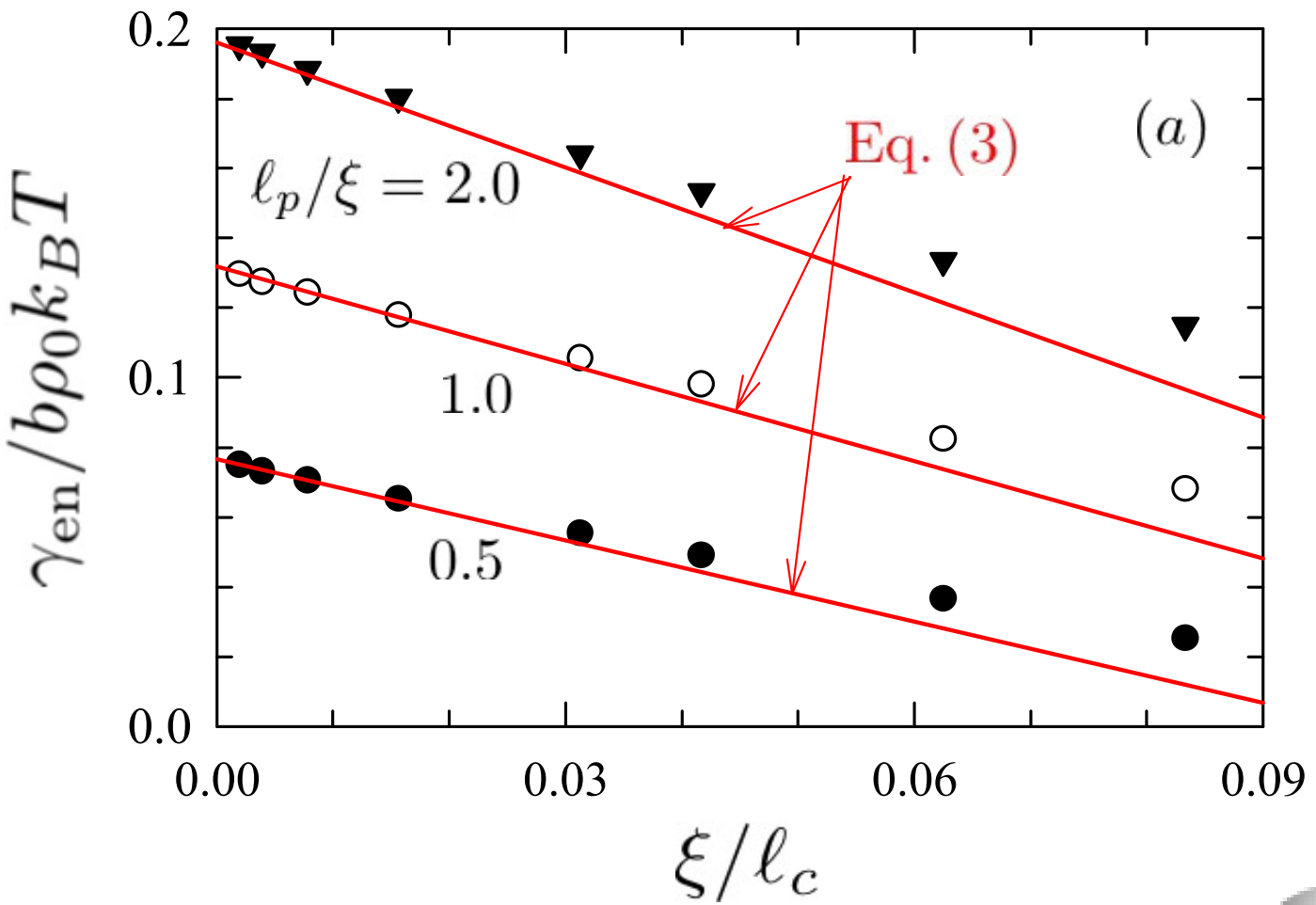
0.2
0.1
0.0
0.00
0.03
0.06
0.09
$\gamma_{\rm en}/b\rho_0 k_B T$
ξ/ℓ_c
$\ell_p/\xi = 2.0$
1.0
0.5
Eq. (3)
(a)

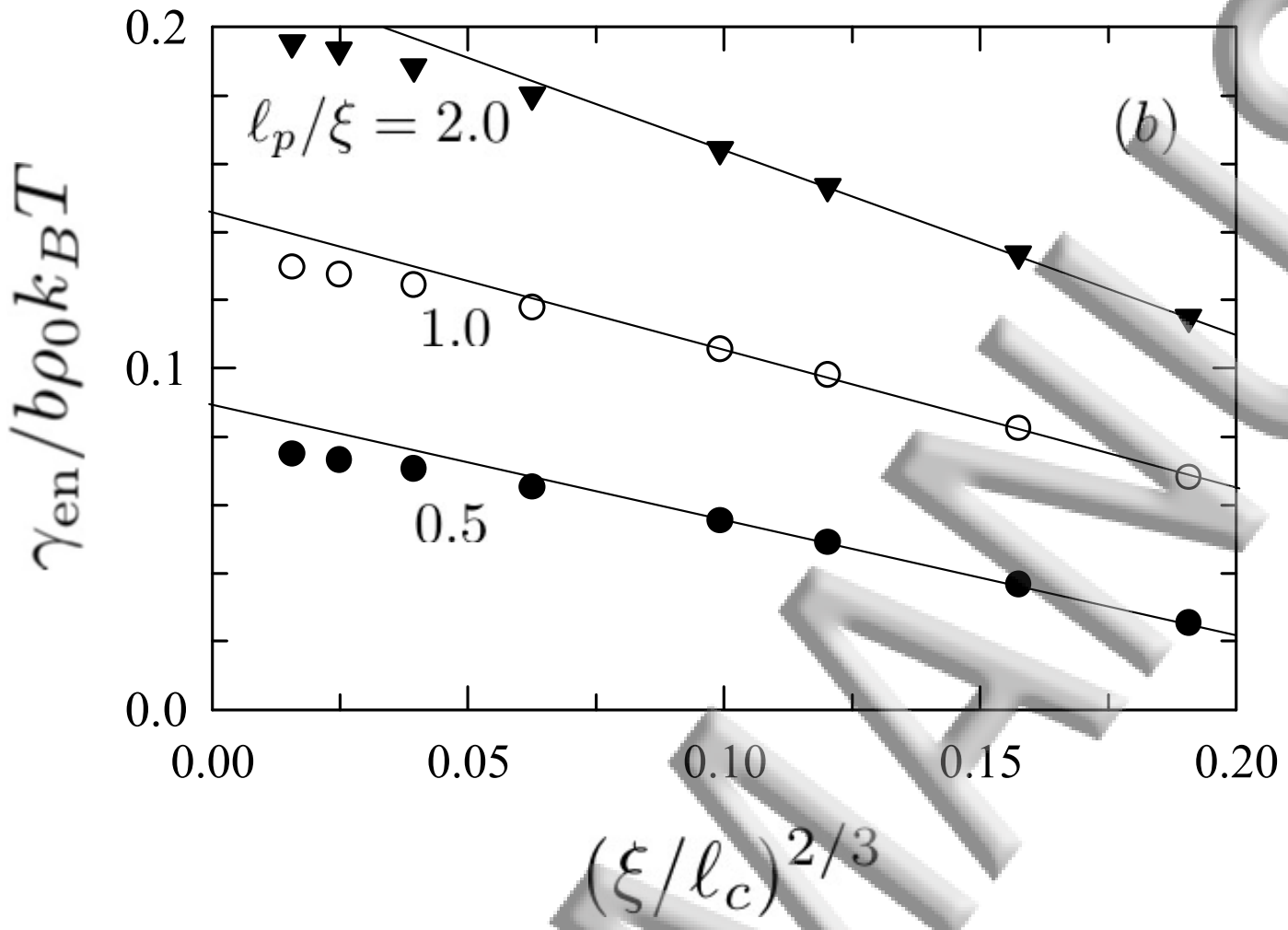
0.2
0.1
0.0
0.00
0.05
0.10
0.15
0.20
$\gamma_{\rm en}/b\rho_0 k_B T$
$(\xi/\ell_c)^{2/3}$
$\ell_p/\xi = 2.0$
1.0
0.5
(b)